Turk J Phys
36 (2012) , 271 – 278.

doi:10.3906/fiz-1105-16

A fresh look at thermal field emission from tungsten tip

Ahmed Abdurrahman Ahmed AL-TABBAKH
Department of Physics, Al-Nahrain University, Baghdad - IRAQ
e-mail: tabbakh2003@yahoo.com

Received: 21.05.2011

Abstract

Electron emission from clean tungsten tips has been investigated at different temperatures and applied electric field. Emission mechanism is analyzed on the basis of the Fowler-Nordheim (FN) model and a parameter extraction model based on elimination of field enhancement factor. The suggested extraction model of the physical and geometrical parameters is found fairly adequate to resolving the apparently confusing behavior of these parameters and shedding light on the emission mechanism. The observed linear FN plots at low temperatures confirm the predominating effect of the applied field on the electron emission. At elevated temperatures, emission is found to fall in the intermediate region between field emission and thermionic emission, therefore known as thermal-field emission.

Key Words: Field electron emission, Fowler-Nordheim theory, parameter extraction model

1. Introduction

Field emission is the emission of the electrons from the condensed phase of metallic or semiconducting materials that are subjected to high electric field into the vacuum [1]. Although the emission occurs by electrons tunnelling through a surface potential barrier that requires no supply of energy to electrons (making the process temperature independent), there has been continuous interest to investigate the effect of temperature elevation on emission mechanism in both metals and semiconductors [2–7]. This interest has recently been motivated by potential applicability of field emitters in high temperature microelectronics [8–10]. In addition, thermal effects are believed to add a new dimension in the interpretation of experimental observations based on theoretical model of Fowler and Nordheim [1]. It is therefore aim of the present work to investigate the field emission characteristics at different temperatures and re-examine the parameter extraction model adopted in conventional interpretation of the data. This paper takes a fresh look at thermal-field emission from clean tungsten tip based on the above mentioned motivations and is also proposed to be available for interested researchers of this re-emerging field.

2. Experimental procedure

Sharp tips of a few hundred nanometres in radii have been prepared by electrochemical etching of fine tungsten wires of high purity (99.9%) [11]. The electrochemical process of etching in this work involves anodic dissolution of the metallic electrode in an electrolytic cell containing 90 g of NaOH dissolved in 100 ml of distilled water (see Figure 1(a, b, c)). The starting diameter of the tungsten wires were 0.1 mm and the ultimate radii of the tips after the etching process are few hundred nanometres, as shown in the scanning electron micrographs (SEMs) of Figure 1(b) and (c).

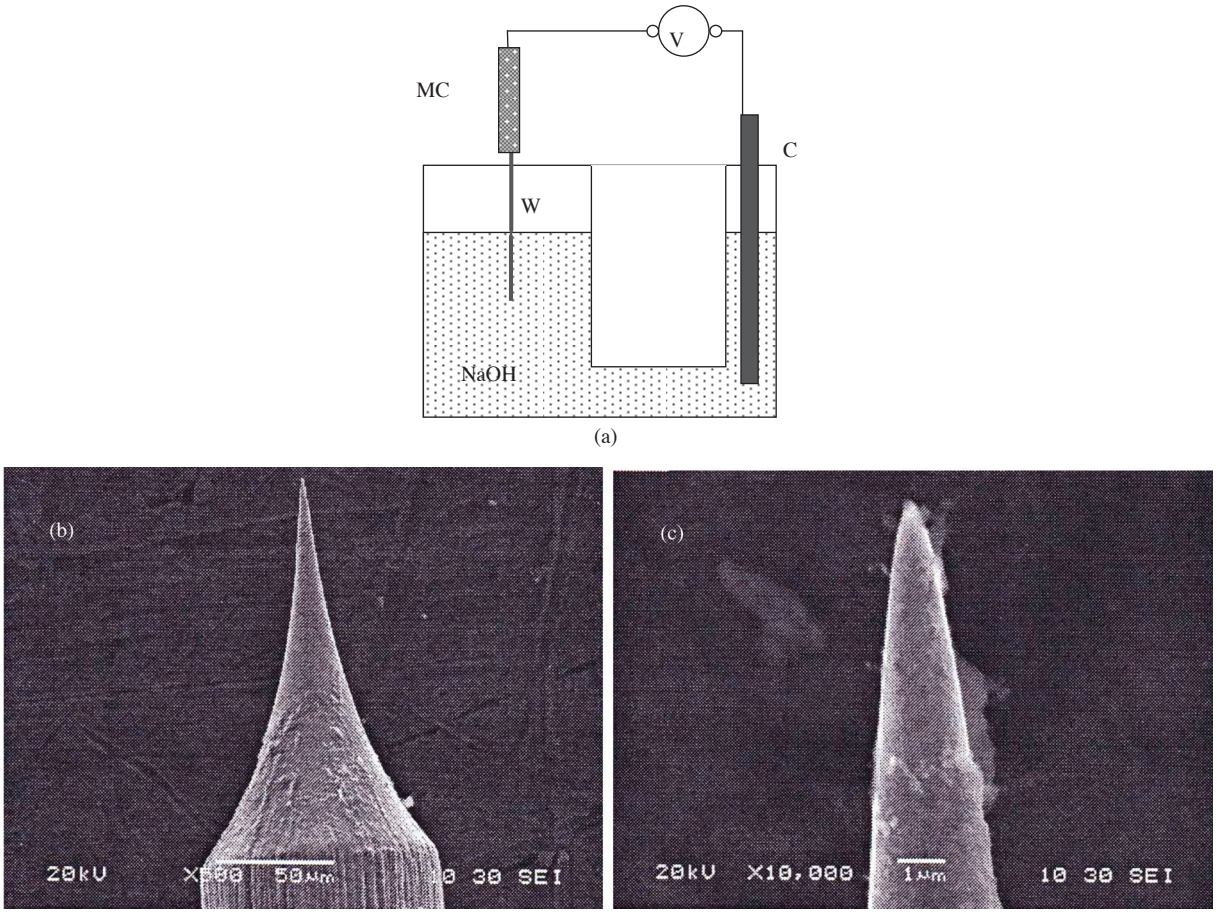

Figure 1. (a) Electrochemical etching/polishing electrolyte for tip fabrication. (c): Counter electrode (carbon), W: Tungsten wire 0.1mm, V: voltage supply, MC: Mechanically-held clamp, HC: Hand-held clamp. (b) and (c) images of SEMs for the tungsten tip at low and high resolutions respectively taken prior to measurements.

Tips are then mounted on tungsten loop provided with two extra coils from the same material so that a four-probe assembly is utilized for both current and voltage measurements and temperature control of the tip. The tip-loop assembly is placed inside a glass envelope that has a conducting and phosphorous screen at the opposite side of the tip (see Figure 2). The glass envelope is evacuated to ultra high vacuum condition. The ultimate pressure, under which all measurements have been achieved, is less than 5×10^{-9} mbar.

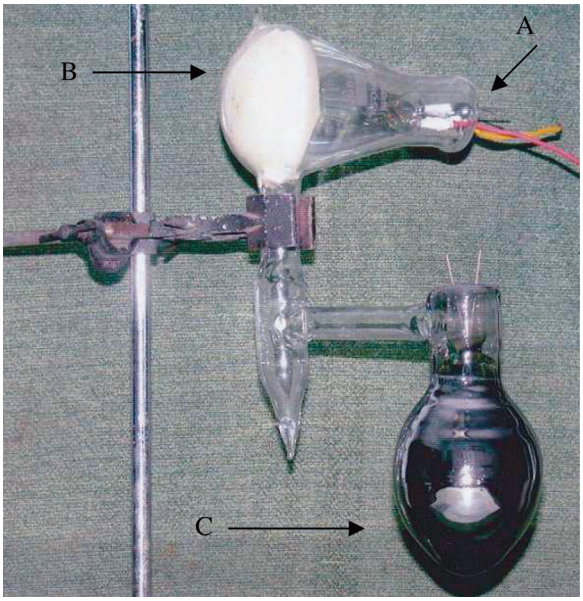

Figure 2. Experimental glass envelope carrying the four-probe tip mounting assembly (A) opposite to a phosphorous conducting screen (B). The label "C" identifies the getter bulb for the maintenance of ultimate vacuum inside the glass envelope.

A high negative voltage is applied to the tip using a, 40 kV, 2 mA Spellman power supply, stabilized to within 0.01%, and the conducting screen is used to collect the emitted electrons, connected to a Keithley 485electrometer. The phosphorous screen is utilized to visualize the pattern of the electronic emission from the surface of the tip projected on it with as high as 10^5 a magnification [12]. That is the ultimate magnification of the field electron microscope. The temperature of the tip is set by using the four-probe method. A variable current is passed through the loop and the voltage drop across the middle coils is registered for each current value. It is therefore possible to measure the resistance of the central part of the loop carrying the tip from the resistivity of the tungsten $(5.25 \times 10^{-8}\ \Omega \cdot m)$. A tip temperature calibration curve is then easy to be determined from the relation between resistance and temperature via the relation

$$R = R_o[1 + \alpha(T - T_o)], \tag{1}$$

where the temperature coefficient $\alpha = 0.0045$ for tungsten. Prior to measurements, a systematic cleaning of tungsten emitters had been achieved by flashing the tungsten loop for short instants of time. This ensured cleaning of the emitter surface of residual gas adsorbents, while preventing the tips from being blunted by atomic migration [13]. Operation of the getter bulb (shown in Figure 2) is attempted to maintain the ultimate vacuum inside the glass envelope.

3. Results and discussion

Current-voltage (I-V) characteristics have been measured for applied voltages of 5 kV to 8.3 kV, so that a generated field is within the effective range for field emission at low temperatures. Figure 3 shows the I-V curve and the corresponding Fowler-Nordheim (FN) plot at room temperature. The FN plot exhibits a linear behaviour, given by the following equation, confirming the metallic nature of the emitting surface and the FN

type emission of electrons [1, 12]:

$$\log\left(\frac{I}{V^2}\right) = -2.9669\times10^7\,\frac{\phi^{3/2}\,f(y)}{\beta\,V} + \log\left(1.54\times10^{-6}\,\frac{\beta^2 A}{\phi\,t^2(y)}\right). \tag{2}$$

Here, $A$is the emitting area, β is the enhancement factor at the emitter surface (β = Electric field/Applied voltage), ϕ is the effective work function, $t(y)$ is a slowly varying function and $f(y)$ is a correction function due to image force approximation. Also, $y = \sqrt{e^3 \cdot F/\phi}$, where F is the average field value at the surface of the emitter. The slope of the straight line is calculated as follows:

$$\text{Slope}_{FN} \equiv m = -6.83\times10^3\frac{\phi^{3/2}S(y)}{\beta} \tag{3}$$

where $S(y)$ is another function of slowly varying value close to unity. From the slope (-5.73 at room temperature) and an average work function of 4.52 eV, a tip radius has been calculated by an iterative method accurate to within five figures and is found equal to 395 nm at $S(y) = 0.993$. A full description of the iterative method is available elsewhere [14]. The field enhancement factor β is assumed equal to $1/5r$ for hemispherical geometry of the tip apex (r is the radius of the hemispherical tip). This value refers to the radius of the effective emitting surface of the tungsten tip.

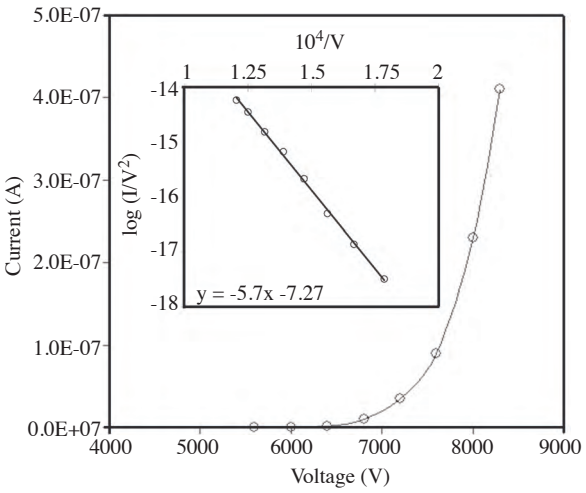

Figure 3. I-V characteristic and FN plot (inset) for clean tungsten tip at room temperature. A straight line behaviour, indicated by the equation in the inset, confirms an FN emission from metallic surface. Tip radius is 395 nm.

Emission patterns were recorded from the phosphorous screen at different temperatures and applied fields for the investigated samples and are shown in Figure 4. The field emission patterns confirm the (110) orientation of the crystal structure at the tip apex as compared with the standard orthographic projection of a hemispherical cubic crystal [12, 15]. Bright regions of the pattern correspond to low work function areas where emission is more probable. Careful examination of the pattern intensity shows how temperature raise of the emitter enhances emission from the low work function areas. This is because the number of electrons near the top of the potential barrier at the emitter surface increases with the energy provided to the electrons inside the

bulk material. In addition, Figure 4 suggests that electron emission from peripheries of planes (100) and (211) enhance due to a build-up process under high field and temperature in agreement with Fujita and Shimoyama [16].

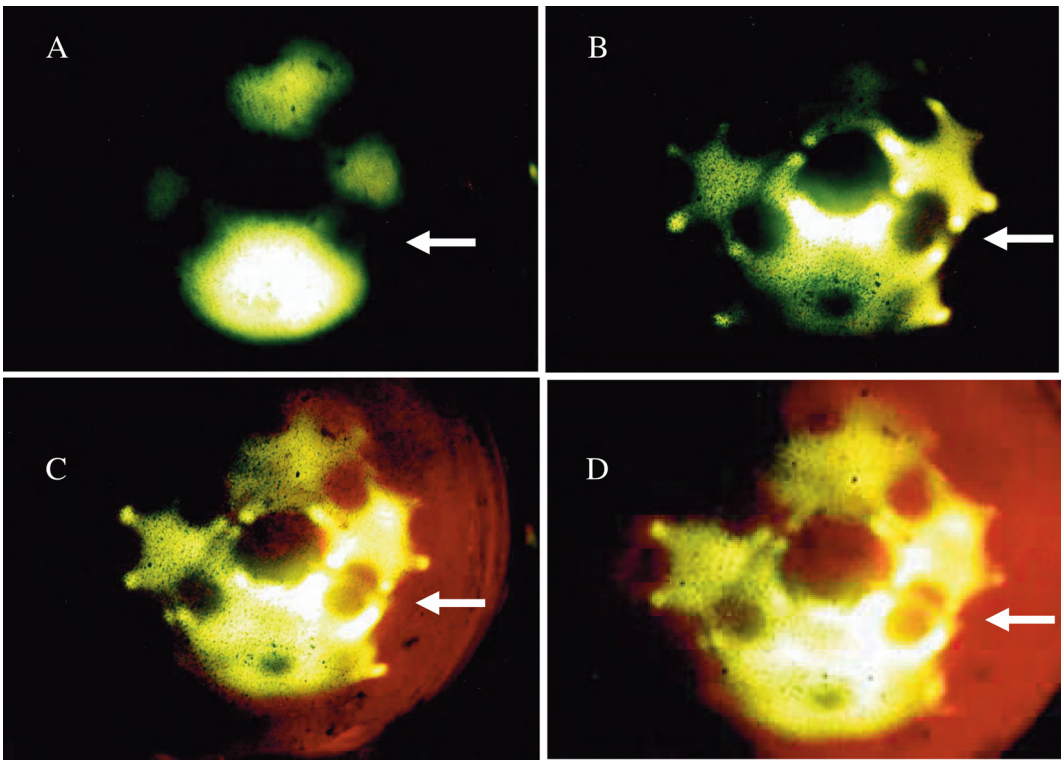

Figure 4. Field emission patterns from clean tungsten tip at different temperatures. (a) 300 K (b) 790 K (c) 1410 K (d) 1920 K. The arrow in each figure refers to grain boundary between two adjacent single crystals at the surface emitter.

Shimoyama and Maruse presented a theoretical investigation of the axial brightness and current density of the emitted electrons as to increase with the rise of field and temperature and decrease with work function values [7]. They showed that temperature effect on axial brightness is much larger at weak fields than the high field. However, no argument has been made on the emission mechanism in terms of the actual emitting area of the material and its dependence on emitter temperature. This will be discussed below.

Further understanding of the emission mechanism is deduced from the FN plots behaviour, the extracted physical and geometrical parameters and the evolution of emission pattern at temperatures higher than the room temperature. For the measurement of the I-V characteristics and corresponding FN plots at elevated temperatures a temperature calibration curve has primarily been obtained from the four-probe method as described earlier and is depicted in Figure 5. The temperature control method is believed to be accurate within 5% error or less. It is therefore possible to set the emitter temperature by applying certain voltages at constant current across the tungsten loop.

FN plots for emitted electrons at elevated temperatures of 790 K, 1410 K and 1920 K were obtained accordingly and are shown in Figure 6. It is possible to describe electron emission fairly well by a certain fit of FN behaviour (linear) for emissions at tip temperatures as high as 1410 K. No deviation from linear behaviour has been observed indicating a dominating field emission from the surface of the tip.

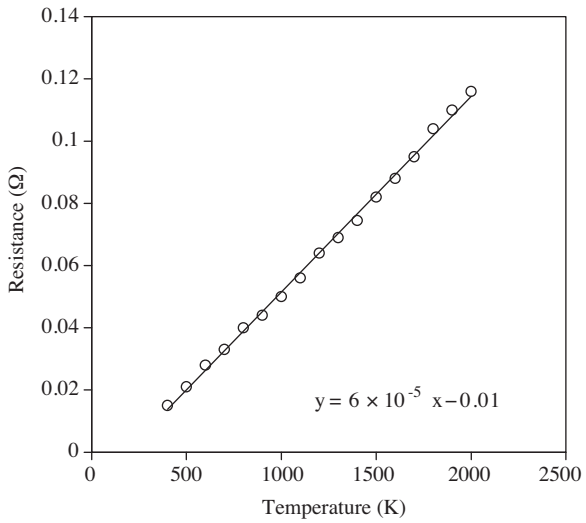

Figure 5. Tip temperature calibration curve of tungsten emitter.

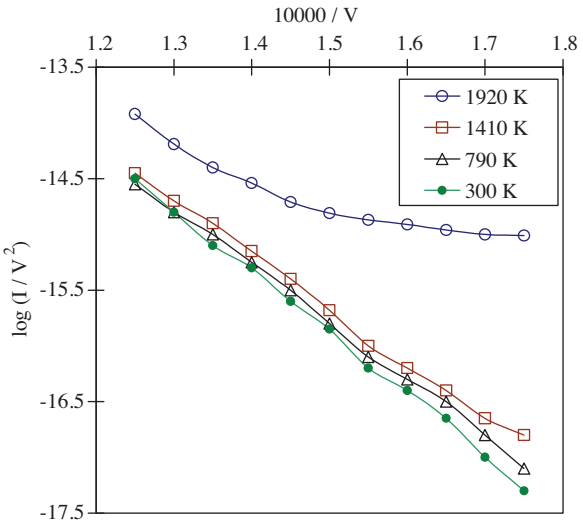

Figure 6. FN plots of field emitted electrons from clean tungsten tip at different temperature showing deviation from FN linear behaviour at higher temperatures.

The slopes of the FN plots, the corresponding intercepts with the vertical axis of the FN plot and the effective radii, as calculated from the iterative method, are shown in Table 1. A careful examination of the table suggests a decrease of the radii of the effective emitting area with the increase of the tip temperature, therefore a decrease of the total emitting area ($A = 2\pi r^2$). In the conventional parameters extraction model (the model used to determine field enhancement factor, average work function of the emitting surface, etc.) the shape of the emitter apex is assumed hemispherical at best approximation [15]. The radius of the hemisphere is approximately determined from the enhancement factor and equation 3 as described above, rather than being measured directly. It is obvious that the hemisphere, approximating the emitting area, vary due to variation of FN plot which depends on the operational conditions of the emitter. Modification of the emitter geometry under influence of field and thermally activated surface has also been investigated by other researchers [15]. However, the reduction of the tip radius with temperature is not well understood in the present investigation and may be caused by overlapping effects overlooked in the parameter extraction model. In addition, an increase of the emission area with the increase of the temperature is observed from the emission patterns of Figure 4. This could be justified by evolution of emission sites from low work function regions of the emitter as described by Fujita and Shimoyama [16].

Table 1. Parameters of Fowler-Nordheim equation for field electron emission at elevated temperatures. m is the slope of the FN plot, b is the intercept. "NA" denotes to cases were fits are not applicable with the parameter extraction model.

T (K)	M	b	R (nm)	A (m^2)	S (y)	$\phi^2 A$
300	-5.7	-7.630	395	9.8033×10^{-13}	0.9927	5.606×10^{-8}
790	-5.08	-8.168	360	8.143×10^{-13}	0.9875	1.29×10^{-8}
1410	-4.86	-8.371	345	7.478×10^{-13}	0.9853	7.4×10^{-9}
1920	NA	NA	NA	NA	NA	NA

To further investigate the dubious situation a model of parameter extraction equation has been suggested by eliminating the field enhancement factor β from the slope (m) and the intercept (b) of the FN equation (equation 2) [17, 18], resulting in the following characteristic equation, which has rarely been used for interpretation of experimental observations:

$$\phi^2 A = \frac{m^2 \times 10^b}{13.584} \tag{4}$$

Equation 4 is advantageous due to elimination of β factor that may, otherwise, add difficulty in resolving the role of the affecting factors in the field emission mechanism. The parameter $\phi^2 A$ is calculated from equation 4 and listed in Table 1, showing a decrease in value with the increase of temperature. Since the factor β does not appear in equation 4, any variation in the equation value should be attributed to either the work function ϕ or the emission area A. And because decrease of emission area could not be justified especially with increasing emitter temperature, it is rather appropriate to attribute the decrease in $\phi^2 A$ to a decrease of work function value. This could be justified by the increase of electron emission from states above the Fermi level which are apparently occupied at higher temperatures. It is therefore reasonable to assume that intensity of emission pattern does not account for a prominent variation in the actual emission area rather than an increase of the number of electrons from an already activated sites of the tip surface. It is shown in Table 1 that, when tip temperature is elevated above 1410 K, a deviation from the linear behaviour of the FN plot is noticed. A fit of the data with an FN-type equation is therefore not plausible (see Figure 6). From the values depicted in Table 1 and the FN plots behaviour of Figure 6 it is reasonable to deduce that size effect has not altered the emission mechanism at elevated temperatures as such effect (observed as deviation from nonlinear behaviour) was still passive at low temperature. This is basically confirmed from the linear behaviour of the FN plots. Therefore, downsizing effect and emitter's temperature are not possibly correlated.

A further understanding of the emission mechanism and the effect of temperature on the FN plot behaviour is possible through energy analysis of the emitted electrons, a task which is beyond the scope of this paper. Nevertheless, a check for the nature of emission, being in thermionic or field emission regimes, is

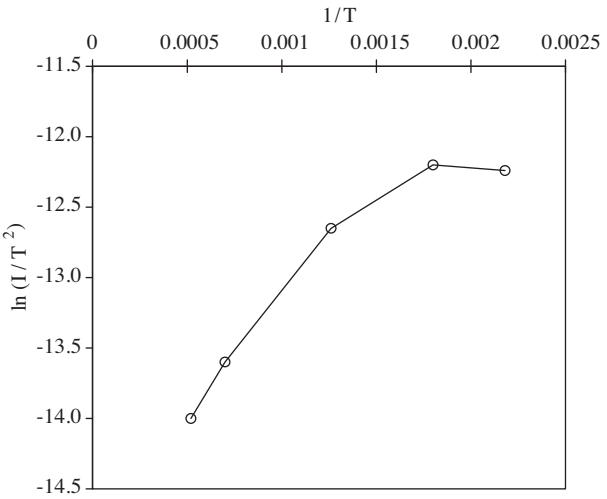

Figure 7. Plot of I-V characteristics on Richardson-Dushman axes. Nonlinear behaviour suggests a thermal-field emission of electrons from the surface of the tungsten tip.

possible by plotting emission currents on Richardson-Dushman axes ($\ln(I/T^2)$ as a function of $1/T$) at constant applied voltage, as shown in Figure 7. The applied voltage on emitter is set to about 6 kV while emission current is measured at different elevated temperatures. If the emission is purely thermionic, a straight line with a slope of negative value is supposed to fit the experimental data in accordance with the Richardson-Dushman equation. However, the nonlinear behaviour of the data and the polarity of the slope being of high positive value, suggests that electron emission is in the intermediate regime between purely field emission and purely thermionic emission, therefore known as thermal-field emission [7, 12]. The deviation from the linearity of the graph could be attributed to contribution of both the field emission electrons and thermionic electrons to the total emission current.

4. Conclusions

Electron emission mechanism from tungsten tips have been investigated at elevated temperatures to shed more light on emission behaviour with reference to FN model and Richardson-Dushman equation. The suggested extraction model of the physical and geometrical parameters is found fairly adequate in resolving the apparently confusing behaviour of these parameters (actual emission area and effective work function) and shedding light on the emission mechanism. The linear behaviour, observed in the FN plots at low temperatures, confirm the predominating effect of the applied field on the electron emission while the size effect on the FN plot behaviour is found unimportant. At elevated temperatures, emission is found to fall in the intermediate region between field emission and thermionic emission, therefore known as thermal-field emission.

References

[1] R. H. Fowler and L. W. Nordheim, *Proc. Roy. Soc. (London),* **A119**, (1928), 173.

[2] F. A. Koch, J. M. Garguilo, B. Brown and R. J. Nemanich, *Diamond and Related Materials*, **11**, (2002), 774.

[3] S. Y. Chen and J. T. Lue, *New J. Phys.*, **4**, (2002), 79.1.

[4] S. H. Shin, T. S. Fisher, D. G. Walker, A.M. Strauss and J. L. Davidson, *J. Vacu. Sci. Technol. B*, **21**, (2003), 587.

[5] K. A. Dean, O. Groening, O. M. Kuttel and L. Schlapbach, *Appl. Phys. Lett.*, **75**, (1999), 18.

[6] W. W. Dolan and W. P. Dyke, *Phys. Rev.,* **95**, (1954), 327.

[7] H. Shimoyama and S. Maruse, *Ultramicroscopy*, **15**, (1984), 239.

[8] K. Jensen, J. Weldon, H. Garcia and A. Zettl, *Nano Lett.,* **7**, (2007), 3508.

[9] S. Saito, *Science*, **278**, (1997), 77.

[10] A. Aviram, *J. American Chem. Soc.,* **110**, (1988), 5687.

[11] A. J. Melmed, *J. Vac. Sci. Technol. B*, **9**, (1991), 601.

[12] G. Fursey, Field Emission in Vacuum Microelectronics, ed. I. Brodie and P. Shwoebel, vol. 1 (Moscow, Russia. 2005, Kluwer Academic / Plenum Publisher) p. 3.

[13] A. Roth, Vacuum Technology, vol.1 (Elsevier Science B. V. 1990), p. 45.

[14] D. S. Joag , PhD Thesis, Department of Physics, University of Poona, Pune 411007, India 1978.

[15] Robert Gomer, Field Emission and Field Ionization, vol.1 (American Institute of Physics, New York. 1993), p.121.

[16] S. Fujita and H. Shimoyama, *Phys. Rev. B* **75**, (2007), 235431.

[17] R. G. Forbes, H. B. Deane, Nabil Hamid and H. S. Sim, *J. Vac. Sci. Technol. B*, **22**, (2004), 3.

[18] F. J. Sheini, A. A. Al-Tabbakh, D. S. Joag and M. A. More, *Iranian Physical Journal*, **2**, (2009), 1.